JOURNAL OF BACTERIOLOGY, Apr. 2007, p. 2805–2812 Vol. 189, No. 7
0021-9193/07/$08.00+0 doi:10.1128/JB.01360-06

A Novel Ferredoxin-Dependent Glutamate Synthase from the Hydrogen-Oxidizing Chemoautotrophic Bacterium *Hydrogenobacter thermophilus* TK-6[▽]

Masafumi Kameya, Takeshi Ikeda, Miyuki Nakamura, Hiroyuki Arai, Masaharu Ishii,* and Yasuo Igarashi

Department of Biotechnology, The University of Tokyo, Yayoi 1-1-1, Bunkyo-ku, Tokyo 113-8657, Japan

Received 28 August 2006/Accepted 9 January 2007

Glutamate synthases are classified according to their specificities for electron donors. Ferredoxin-dependent glutamate synthases had been found only in plants and cyanobacteria, whereas many bacteria have NADPH-dependent glutamate synthases. In this study, *Hydrogenobacter thermophilus*, a hydrogen-oxidizing chemoautotrophic bacterium, was shown to possess a ferredoxin-dependent glutamate synthase like those of phototrophs. This is the first observation, to our knowledge, of a ferredoxin-dependent glutamate synthase in a nonphotosynthetic organism. The purified enzyme from *H. thermophilus* was shown to be a monomer of a 168-kDa polypeptide homologous to ferredoxin-dependent glutamate synthases from phototrophs. In contrast to known ferredoxin-dependent glutamate synthases, the *H. thermophilus* glutamate synthase exhibited glutaminase activity. Furthermore, this glutamate synthase did not react with a plant-type ferredoxin (Fd3 from this bacterium) containing a [2Fe-2S] cluster but did react with bacterial ferredoxins (Fd1 and Fd2 from this bacterium) containing [4Fe-4S] clusters. Interestingly, the *H. thermophilus* glutamate synthase was activated by some of the organic acids in the reductive tricarboxylic acid cycle, the central carbon metabolic pathway of this organism. This type of activation has not been reported for any other glutamate synthases, and this property may enable the control of nitrogen assimilation by carbon metabolism.

Glutamate synthase (glutamine:2-oxoglutarate amidotransferase [GOGAT]) is known to be one of the most important enzymes for ammonium assimilation. This enzyme synthesizes Glu from Gln and 2-oxoglutarate (2-OG) as follows: Gln + 2-OG + reduced electron carrier → 2 Glu + oxidized electron carrier.

GOGAT couples with glutamine synthetase (GS) for ammonium assimilation, and their total reaction incorporates NH_3 into 2-OG at the expense of ATP and reducing power. This coupling reaction is called the GS/GOGAT pathway, a prevailing ammonium assimilatory pathway among many organisms (15, 22).

GOGATs are classified into several types according to their specificities for electron donors (27). The first type is ferredoxin-dependent GOGAT (Fd-GOGAT), which utilizes a reduced ferredoxin as an electron donor. Because Fd-GOGAT is found only in cyanobacteria and chloroplasts of plants and is not found in nonphotosynthetic organisms, it is often called "plant-type GOGAT." Another type of GOGAT utilizes NADPH as an electron donor. NADPH-dependent GOGAT (NADPH-GOGAT) is common among most bacteria and is often referred to as "bacterial GOGAT."

Fd-GOGAT is a monomeric protein with a molecular mass of ≈150 kDa, while NADPH-GOGAT forms an $(\alpha\beta)_4$ heterooctamer with α subunits of ≈150 kDa and β subunits of ≈50 kDa. Fd-GOGAT and the α subunit of NADPH-GOGAT are homologous to each other. There is an insertion of ≈18 amino acid residues conserved in Fd-GOGATs from phototrophs but not in reported NADPH-GOGATs. This insertion is called the Fd loop and is suspected to be involved in ferredoxin–Fd-GOGAT binding (26, 27, 28). However, the function of this loop has not yet been clarified, and it remains unclear whether this loop actually contributes to ferredoxin–Fd-GOGAT association. Since no clear differences other than the Fd loop have been found between the primary structures of Fd-GOGAT and the α subunit of NADPH-GOGAT, it cannot be predicted from the gene sequence whether the gene product reacts with ferredoxin or NADPH.

Kinetic properties and tertiary structures of Fd-GOGATs and NADPH-GOGATs have been studied thoroughly (6, 21, 26, 29), showing that both enzymes have similar reaction mechanisms. Fd-GOGAT and the α subunit of NADPH-GOGAT consist of four domains, called the glutamine amidotransferase (GAT) domain, central domain, synthase domain, and β-helical domain. Gln is hydrolyzed at the GAT domain, and the generated ammonia is transferred to the synthase domain through an intramolecular ammonia channel. The ammonia channel is mainly composed of residues of the central and β-helical domains and prevents leakage of ammonia from the enzyme. Transferred ammonia reacts at the synthase domain together with 2-OG and reducing power to produce Glu. Fd-GOGAT and the α subunit of NADPH-GOGAT receive electrons from reduced ferredoxin and the β subunit, respectively.

Hydrogenobacter thermophilus TK-6 is a thermophilic, hydrogen-oxidizing, chemoautotrophic bacterium. Analysis of the 16S rRNA sequence showed that *Hydrogenobacter* species are located on the deepest branch in the domain *Bacteria* in the phylogenic tree, along with *Aquifex* species (20). Owing to its

* Corresponding author. Mailing address: Department of Biotechnology, The University of Tokyo, Yayoi 1-1-1, Bunkyo-ku, Tokyo 113-8657, Japan. Phone: (81)-3-5841-5143. Fax: (81)-3-5841-5272. E-mail: amishii@mail.ecc.u-tokyo.ac.jp.

▽ Published ahead of print on 19 January 2007.

unique evolutionary lineage, many interesting metabolic characteristics have been found. *H. thermophilus* has hydrogenases and utilizes hydrogen as the sole source of energy and reducing power (9). With regard to carbon metabolism, it is known that *H. thermophilus* exhibits obligate autotrophy, fixing carbon dioxide as the sole carbon source through the reductive tricarboxylic acid (RTCA) cycle (24). Key enzymes of this metabolic pathway have been investigated in detail (2, 3, 4, 7, 30). However, less progress has been reported with regard to nitrogen anabolism, except for the identification of GS (10). In this study, we investigated the enzyme that couples with GS and sustains ammonium assimilation in *H. thermophilus* and found an enzyme that catalyzes the GOGAT reaction. We revealed that this enzyme is not a bacterial GOGAT but is a plant-type GOGAT, although *H. thermophilus* is a chemoautotroph, and that the enzyme has some novel features different from those of other plant-type GOGATs.

MATERIALS AND METHODS

Bacterial strains and growth conditions. *Hydrogenobacter thermophilus* TK-6 (IAM 12695, DSM 6534) was cultivated at 70°C as previously described (23). The culture medium contained 3 g/liter $(NH_4)_2SO_4$ as the sole nitrogen source. *Escherichia coli* BL21(DE3) was used as a host for heterologous expression of ferredoxins.

NAD(P)H-GOGAT assay. NAD(P)H-GOGAT activity was determined by measuring the decrease in NAD(P)H and the production of Glu. The reaction mixtures contained 20 mM $NaPO_4$ (pH 8.0), 10 mM Gln, 5 mM 2-OG, 0.3 mM NADPH or NADH, and the enzyme solution in a total volume of 2 ml. Assays were carried out at 70°C under an Ar gas phase. The decrease in NAD(P)H was monitored at 340 nm, using an extinction coefficient of 6.2 $mM^{-1} \cdot cm^{-1}$. Glu production was also measured by a Glu determination method (see below). For activation of NAD(P)H-GOGAT activity by flavin mononucleotide (FMN) and flavin adenine dinucleotide (FAD), 0.2 mM FMN and 0.2 mM FAD were added to the reaction mixtures or the enzyme solution.

Fd-GOGAT assay. Fd-GOGAT activity was determined by measuring the production of Glu and the decrease in 2-OG. When Glu production was measured, the reaction mixtures contained 20 mM $NaPO_4$ (pH 7.2), 10 mM Gln, 1 mM 2-OG, 5 mM methylviologen, 5 mM dithionite, and the enzyme solution in a total volume of 500 μl. When the 2-OG decrease was measured, the reaction mixtures contained 20 mM $NaPO_4$ (pH 7.2), 10 mM Gln, 0.5 mM 2-OG, 5 mM methylviologen, 5 mM dithionite, and the enzyme solution in a total volume of 500 μl. Dithionite and the enzyme solution were added to the mixtures after the gas phase was replaced with Ar. The reaction mixtures were incubated at 70°C for 30 min. The production of Glu and the decrease in 2-OG were measured by methods described below. One unit of activity was defined as the activity producing 1 μmol of Glu or consuming 0.5 μmol of 2-OG per minute. It was confirmed that the initial velocity was sustained during the incubation period. When GOGAT activity was evaluated by Glu production, the difference in the amounts of Glu synthesized in the presence or absence of dithionite was used to calculate the specific activity. Reactivity against various artificial electron carriers and ferredoxins of *H. thermophilus* was evaluated by replacing 5 mM methylviologen with 5 mM benzylviologen, 5 mM methylene blue, 10 μM Fd1, 10 μM Fd2, or 10 μM Fd3. Optimum pH was examined by using $NaPO_4$ or HEPES-KOH at various pHs as a buffer. Activation by organic acids was evaluated by adding 5 mM succinate, oxaloacetate, malate, citrate, isocitrate, fumarate, or pyruvate to the reaction mixtures. These organic acids were neutralized by NaOH to pH 7 prior to the assay. For determination of K_m values for Gln and 2-OG, the concentration of each substrate was varied from 0.4 mM to 10 mM and from 0.08 mM to 1 mM, respectively, using methylviologen as an electron carrier. For determination of the K_m value for Fd1, the concentration of Fd1 was varied from 1 to 10 μM. To exclude the effect of glutaminase activity, GOGAT activity was estimated by the decrease in 2-OG for K_m determination.

Glutaminase assay. Glutaminase activity was determined by measuring Glu production. The reaction mixtures contained 20 mM $NaPO_4$ (pH 7.2), 10 mM Gln, and the enzyme solution in a total volume of 100 μl. The reaction mixtures were incubated at 70°C for 30 min. Since aerobic conditions did not affect the activity, incubation was performed aerobically. The production of Glu was measured by methods described below. Activation by organic acids was evaluated by adding 5 mM succinate, oxaloacetate, malate, citrate, isocitrate, fumarate, pyruvate, or 2-OG to the reaction mixtures.

Glu determination. The Glu concentration was determined by reverse-phase high-performance liquid chromatography (HPLC) after phenylthiocarbamyl derivatization (5). Ala was added to samples as an internal standard, and the samples were dried under a vacuum. Dried samples were dissolved in 10 μl of ethanol-water-triethylamine-phenylisothiocyanate (7:1:1:1) and were left to stand for 10 min. Subsequently, they were dried again under a vacuum. Dried samples were dissolved in an appropriate volume of 25 mM $NaPO_4$ (pH 6.5) and analyzed with a reverse-phase column (Inertsil ODS-3 [4.6 mm by 250 mm]; GL Science, Tokyo, Japan). Derivatized amino acids were eluted according to the gradient, using 25 mM $NaPO_4$ (pH 6.5) and 70% methanol as two eluents. The elution was monitored at 254 nm, using an L-2400 UV detector (Hitachi, Tokyo, Japan), for determination of derivatized amino acids.

2-OG determination. The 2-OG concentration was determined by using glutamate dehydrogenase from beef liver (Oriental Yeast, Tokyo, Japan). For deproteinization, 110 μl of sample was mixed with 12 μl of 50% trichloroacetate and then centrifuged. The supernatant was neutralized with 54 μl of 2 M Tris-HCl (pH 8.0) and used to make up 250-μl reaction mixtures that contained 50 mM $NaPO_4$ (pH 7.2), 0.2 mM NADH, 10 mM NH_4Cl, and 3 U/ml glutamate dehydrogenase. The decrease in NADH was determined by measuring the absorbance at 340 nm. The accuracy of 2-OG determination was validated using standard 2-OG.

GOGAT purification. *H. thermophilus* TK-6 cells were harvested at 5,000 × *g* for 10 min when the optical density at 540 nm reached approximately 2.5. The cells (70 g of wet cells) were washed with 20 mM Tris-HCl buffer (pH 8.0) and disrupted by sonication. Cell debris was removed by centrifugation at 100,000 × *g* for 1 h. The supernatant (designated the cell extract [CFE]) was applied to a DE52 open column (25 mm by 15 cm; Whatman, Brentford, United Kingdom) equilibrated with 20 mM Tris-HCl buffer (pH 8.0) containing 1 mM $MgCl_2$. After elution of bound proteins with buffer containing 1 M NaCl, ammonium sulfate was added to the obtained fraction to 30% saturation, and the sample was applied to a butyl-Toyopearl column (22 mm by 15 cm; Tosoh, Tokyo, Japan) equilibrated with 20 mM Tris-HCl buffer (pH 8.0) containing 1 mM $MgCl_2$ and ammonium sulfate at 30% saturation. This and subsequent chromatography steps were performed using an ÄKTA purifier system (GE Healthcare, Piscataway, NJ). Proteins were eluted with a gradient of ammonium sulfate from 30% to 0% over 230 ml at a flow rate of 4 ml min^{-1}. The active fractions were dialyzed against 20 mM Tris-HCl buffer (pH 8.0) containing 1 mM $MgCl_2$ and were applied to a DEAE-Toyopearl column (22 mm by 15 cm; Tosoh) equilibrated with 20 mM Tris-HCl buffer (pH 8.0) containing 1 mM $MgCl_2$. Proteins were eluted with a gradient of NaCl from 0 M to 1 M over 380 ml at a flow rate of 4 ml min^{-1}. The active fractions were applied to a hydroxyapatite SH-0710 M column (7.5 mm by 10 cm; Pentax, Tokyo, Japan) equilibrated with 1 mM KPO_4 buffer (pH 7.0). Proteins were eluted with a gradient of KPO_4 buffer from 1 mM to 400 mM over 25 ml at a flow rate of 1 ml min^{-1}. The active fractions were dialyzed against 20 mM Tris-HCl buffer (pH 8.0) containing 1 mM $MgCl_2$ and were applied to a MonoQ HR 5/5 column (GE Healthcare) (bed volume, 1 ml) equilibrated with 20 mM Tris-HCl buffer (pH 8.0) containing 1 mM $MgCl_2$. Proteins were eluted with a gradient of NaCl from 0 M to 1 M over 40 ml at a flow rate of 0.5 ml min^{-1}. The active fractions were designated purified GOGAT and stored at −80°C until use.

Construction of expression plasmid for Fd3. The *fdx3* gene was amplified by PCR from the chromosomal DNA of *H. thermophilus*, using a pair of primers, namely, 3F (5′-AGAATAAAAACATATGGCAAAGGTA-3′), which introduced an NdeI site (underlined) at the initiation codon, and 3R (5′-TC*GAATT C*TCAATCAGTTTCTA), which introduced an EcoRI site (in italics) after the stop codon. The obtained PCR product was digested with NdeI and EcoRI and ligated with NdeI-EcoRI-digested pET21c. The nucleotide sequence of the inserted fragment was confirmed on both strands. The resultant plasmid was designated pET-Fd3.

Heterologous expression and purification of ferredoxins. Three ferredoxins of *H. thermophilus*, namely, Fd1, Fd2, and Fd3, were expressed in *E. coli* and purified by heat treatment, Q Sepharose fast-flow chromatography, and Superdex 75 HR 10/30 chromatography as previously described (8). Fd3 was further purified on a MonoQ column; the Superdex 75 fractions containing Fd3 were pooled and loaded onto a MonoQ column equilibrated with 20 mM Tris-HCl buffer (pH 8.0) containing 1 mM $MgCl_2$. Proteins were eluted with sequential linear gradients from 0 M to 0.2 M NaCl over 5 ml and from 0.2 M to 0.4 M NaCl over 30 ml at a flow rate of 1 ml min^{-1}.

N-terminal amino acid sequencing. The N-terminal amino acid sequences of GOGAT and Fd3 were determined by Procise 491cLC or 492HT (Applied

TABLE 1. Purification of GOGAT from *H. thermophilus* TK-6

Fraction	Total activity (U)	Total amt of protein (mg)	Sp act (U/mg)	Purification factor (fold)	Yield (%)
CFE	19	2,443	0.0078	1	100
Butyl Toyopearl	9.0	197	0.046	6	47
DEAE Toyopearl	4.9	12	0.40	52	26
Hydroxyapatite	2.0	3.7	0.54	69	10
MonoQ	0.91	0.61	1.5	191	4.7

Biosystems, Foster City, CA) from a blotted membrane (0.2-μm Sequi-Blot polyvinylidene difluoride membrane; Bio-Rad, Hercules, CA).

Protein assay. Protein concentrations were measured using a BCA protein assay kit (Pierce, Rockford, IL) or an *RC DC* protein assay kit (Bio-Rad). A calibration curve was plotted using bovine serum albumin as a standard protein.

Gel filtration. For estimation of the molecular mass, gel filtration was performed using a Superose 6 HR 10/30 column (GE Healthcare) equilibrated with 20 mM Tris-HCl (pH 8.0) buffer containing 1 mM $MgCl_2$ and 150 mM NaCl at a flow rate of 0.5 ml min^{-1}. Chromatography was performed using an ÄKTA purifier system. A gel filtration standard (Bio-Rad) was used as molecular markers for the calibration. Each measurement of standards or samples was performed in triplicate.

Flavin determination. Flavin content was determined by reverse-phase HPLC after trichloroacetate treatment (11, 13). Calibration curves were constructed using standard FMN and FAD that were subjected to the same procedure.

Spectroscopic measurements. UV-visible spectra were measured on a Beckman DU 7400 spectrophotometer (Beckman Coulter, Fullerton, CA). Electron paramagnetic resonance (EPR) spectra were measured on a JEOL JES-FA300 spectrometer equipped with an ES-CT470 cryostat system and a digital temperature indicator/controller (Scientific Instruments, West Palm Beach, FL).

Construction of phylogenetic tree. Amino acid sequences were aligned using Clustal X 1.83. After removal of the upstream regions of the N-terminal Cys residues, a phylogenetic tree was constructed by the neighbor-joining method, using Mega 3.1.

Nucleotide sequence accession numbers. The nucleotide sequences of *gltS* and *fdx-3* have been deposited in the DDBJ/EMBL/GenBank nucleotide sequence database under accession numbers AB269904 and AB269905, respectively.

RESULTS

Purification of GOGAT from *H. thermophilus*. It was previously demonstrated that *H. thermophilus* has GS (10), suggesting the presence of enzymes that catalyze the GOGAT reaction. NADPH- or NADH-dependent GOGAT activity in CFE of *H. thermophilus* was assayed by two detection methods, namely, measuring the decrease in NAD(P)H photometrically and measuring the production of Glu by HPLC. No NAD(P)H decrease that depended on both Gln and 2-OG was detected. Although Glu synthesis was observed when Gln was present in reaction mixtures (0.02 μmol $min^{-1} \cdot$ mg of $protein^{-1}$), this Glu synthesis depended on neither 2-OG nor NAD(P)H. These results indicated that *H. thermophilus* does not have NADPH- or NADH-dependent GOGAT activity but has glutaminase activity, which hydrolyzes Gln to Glu and ammonium. Activation by FMN and FAD was also tested because NADPH- and NADH-dependent GOGATs are known to be flavoproteins containing FMN and FAD, but their activities remained undetectable even after the activation treatment. When NAD(P)H was replaced with dithionite-reduced methylviologen, Glu production increased 1.5-fold, to 0.03 μmol $min^{-1} \cdot$ mg of $protein^{-1}$. The activity depended on all of the constituents (i.e., 2-OG, methylviologen, and dithionite), suggesting that GOGAT activity was present in the CFE. Thus, we performed a purification of the enzyme that synthesizes Glu from Gln and 2-OG, using reduced methylviologen as an electron donor.

From 70 g of wet cells, 0.61 mg of the enzyme was obtained (Table 1). Neither NADPH- nor NADH-dependent GOGAT activity was detected throughout the purification. The purified enzyme gave a single band of 151 kDa by sodium dodecyl sulfate-polyacrylamide gel electrophoresis (SDS-PAGE) (Fig. 1). The N-terminal amino acid sequence was CGVGFVCNIR. This amino acid sequence agreed entirely with the product of a gene (designated *gltS*) in the draft genome data of *H. thermophilus* (unpublished data). No genes other than *gltS* were found to encode this amino acid sequence. *gltS* is homologous to genes encoding Fd-GOGAT and the α subunit of NADPH-GOGAT. Met codons are present six and eight residues upstream of the N-terminal Cys codon, suggesting that cleavage of the GOGAT prepeptide occurs in *H. thermophilus* as well as in Fd-GOGATs and NADPH-GOGATs from other organisms (17, 18, 19). The calculated molecular mass was 168 kDa, which is in accordance with that estimated by SDS-PAGE. GltS of *H. thermophilus* conserves putative regions for FMN binding and [3Fe-4S] cluster formation in reported GOGATs (27), suggesting the presence of FMN and iron-sulfur clusters as well as other GOGATs (see below).

It is known that NADPH-GOGATs from other organisms have a β subunit and that genes encoding α and β subunits are adjacent in the genome. No genes encoding a β subunit of NADPH-GOGAT were found upstream or downstream of *gltS* in the genome of *H. thermophilus* (data not shown), providing further evidence that this enzyme lacks reactivity toward NADPH.

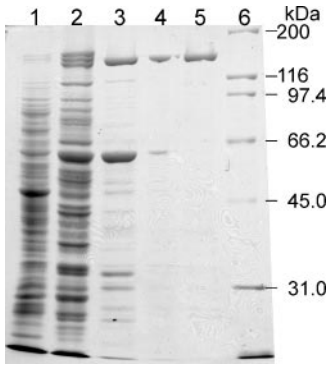

FIG. 1. SDS-PAGE (10%) analysis of GOGAT purification fractions. Lane 1, CFE (27 μg); lane 2, butyl-Toyopearl fraction (23 μg); lane 3, DEAE-Toyopearl fraction (4 μg); lane 4, hydroxyapatite fraction (1.5 μg); lane 5, MonoQ fraction (1.5 μg); lane 6, molecular mass markers (1 μg of each).

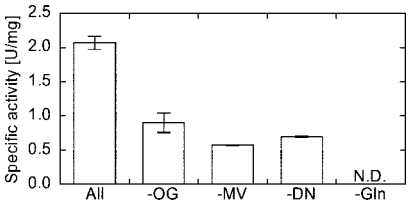

FIG. 2. Glu production activities in reaction mixtures with all substrates and electron donors and in those lacking one of them. Error bars indicate standard errors for at least three independent experiments. OG, 2-oxoglutarate; MV, methylviologen; DN, dithionite; N.D., not detected.

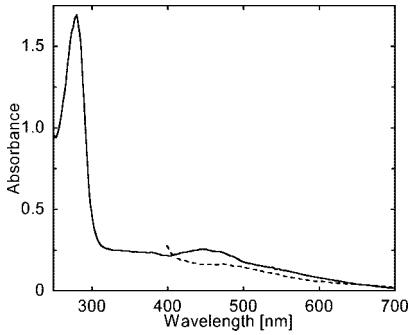

FIG. 3. UV-visible spectra of Fd-GOGAT in the air-oxidized state (solid line) and in the dithionite-reduced state (dotted line).

To determine the subunit composition, gel filtration was performed. The native molecular mass was estimated to be 115 kDa, suggesting that the enzyme is a monomer, as in the case of Fd-GOGATs from phototrophs. The subsequent SDS-PAGE analysis confirmed that the enzyme was not degraded during the gel filtration process. The molecular mass estimated by gel filtration was smaller than that determined by SDS-PAGE or by the deduced amino acid sequence, which might be due to the compact folding peculiar to proteins from thermophiles.

On the basis of the amino acid sequence and subunit composition described above, it is suggested that the structure of the enzyme is similar to that of Fd-GOGATs from phototrophs.

Enzymatic properties. The substrate dependency of Glu production was determined using the purified enzyme (Fig. 2). Glu was produced at 0.6 μmol min^{-1} · mg of $protein^{-1}$, even when the reaction mixture contained only Gln as the sole substrate, indicating that the purified enzyme also has glutaminase activity. When all substrates and electron donors were present in the reaction mixture, Glu production increased to 2.1 μmol min^{-1} · mg of $protein^{-1}$, indicating 1.5 U/mg of protein of GOGAT activity. A nearly stoichiometric decrease in 2-OG at the rate of 0.8 μmol min^{-1} · mg of $protein^{-1}$, corresponding to 1.6 U/mg of protein, was also detected. This decrease was observed only when Gln, 2-OG, methylviologen, and dithionite were present. These data show that the purified enzyme has GOGAT activity using methylviologen as an electron carrier.

The air-oxidized enzyme showed a UV-visible spectrum similar to those for reported Fd-GOGATs in the visible region (13), with an A_{280}/A_{440} ratio of 7 (Fig. 3). The peak around 440 nm disappeared after the addition of dithionite under anaerobic conditions, suggesting the reduction of flavin and iron-sulfur clusters. In flavin analysis, FMN was detected in the enzyme extract, while no FAD was detected. The FMN content ratio was calculated to be 0.9 ± 0.1 mol of FMN per mol of protein, indicating a ratio of one FMN per protein, as in the case of reported Fd-GOGATs (13). These results suggest that FMN and iron-sulfur clusters were functionally present in the purified enzyme as well as in other GOGATs.

Fd3 preparation. Although it was shown that the purified enzyme has reactivity against methylviologen, this enzyme was expected to react with natural electron carriers, such as ferredoxins. Ferredoxins are classified into several groups according to the structure of their iron-sulfur clusters. Ferredoxins that contain a [2Fe-2S] cluster are prevalent in plants, and they are called plant-type ferredoxins. Fd-GOGATs from phototrophs are reported to react with [2Fe-2S] ferredoxins (13). Two [4Fe-4S] ferredoxins (Fd1 and Fd2) have been found in *H. thermophilus*, and they were purified from recombinant *E. coli* (8). From the draft genome data, a novel ferredoxin gene, *fdx3* (encoding Fd3), was found in the genome of *H. thermophilus.* The deduced amino acid sequence for *fdx3* was 70.2% identical to that for *Aquifex aeolicus fdx1*, which encodes a plant-type ferredoxin containing a [2Fe-2S] cluster (16). The gene product of *H. thermophilus fdx3* contains conserved cysteine residues that serve as probable ligands for an iron-sulfur cluster. In order to investigate the reactivity of GOGAT with Fd3, along with Fd1 and Fd2, we performed heterologous expression and purification of Fd3.

Recombinant Fd3 was expressed in *E. coli* and was purified to homogeneity. The N-terminal amino acid sequence of purified Fd3 was AKVKI, indicating that the first Met was removed by posttranslational modification. The UV-visible spectrum of air-oxidized Fd3 showed maxima at ca. 550, 460, 420, and 350 nm (Fig. 4), which are characteristic of ferredoxins containing a [2Fe-2S] cluster. The A_{420}/A_{280} ratio for Fd3 was approximately 0.58. Upon the addition of dithionite under anaerobic conditions, the absorbance decreased over the whole visible range, indicating that the [2Fe-2S] cluster of Fd3 was reduced by dithionite. In the dithionite-reduced state, Fd3 showed a simple, rhombic EPR spectrum ($g_{z,y,x}$ = 2.05, 1.95, and 1.89), which is attributed to the $S = 1/2$ $[2Fe\text{-}2S]^{+}$ cluster (Fig. 5). The *g* values are analogous to the rhombic resonances observed for plant-type ferredoxins and distinct from those for the axial EPR spectra that are characteristic of the mammalian adrenodoxin-like, bacterial putidaredoxin-like, and bacterial

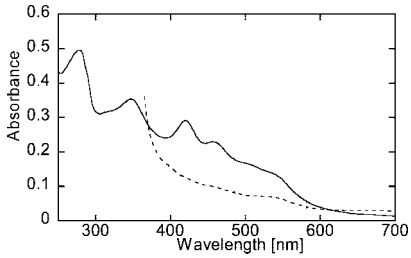

FIG. 4. UV-visible spectra of recombinant Fd3 in the air-oxidized state (solid line) and in the dithionite-reduced state (dotted line).

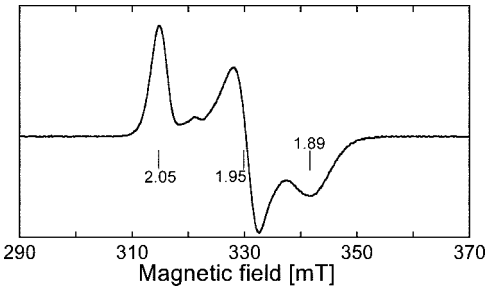

FIG. 5. Low-temperature EPR spectrum of recombinant Fd3 in the dithionite-reduced state. Instrument settings for EPR spectroscopy were as follows: temperature, 10 K; microwave power, 0.05 mW; microwave frequency, 9.026 GHz; modulation frequency, 100 kHz; modulation amplitude, 0.2 mT. The *g* values are indicated.

Isc ferredoxins (32). These results show that purified Fd3 retained the functional conformation of its [2Fe-2S] cluster.

Reactivity with electron carriers. Reactivities of GOGAT with Fd1, Fd2, and Fd3 were compared by measuring the Glu-producing activity (Fig. 6). GOGAT activity was detected when Fd1 or Fd2 was used as an electron carrier and was slightly higher (up to 140%) than that with methylviologen. In contrast, when Fd3 was used as an electron carrier, no significant GOGAT activity was detected. These results indicate that [4Fe-4S]-type Fd1 and Fd2 react with GOGAT more efficiently than does methylviologen, while [2Fe-2S]-type Fd3 does not.

Reactivities with artificial electron carriers other than methylviologen were also investigated. When benzylviologen was used, GOGAT activity decreased to one-sixth the activity with methylviologen. No GOGAT activity was detected when methylene blue was used. GOGAT activity was not detected when NADPH or NADH was added as an electron donor, confirming that the enzyme has no reactivity with NADPH or NADH.

Glu production in these reaction mixtures coincided with 2-OG consumption (data not shown), confirming the results described above.

Kinetic characterization. Purified Fd-GOGAT exhibited Michaelis-Menten kinetics with Gln and 2-OG, and the K_m values for Gln and 2-OG were estimated to be 1.1 mM and 0.28 mM (V_{max}, 1.5 U/mg of protein and 2.0 U/mg of protein), respectively. The reactivity with specific ferredoxins was also investigated, and the results showed no significant difference between reactivities with Fd1 and Fd2. The K_m value for Fd1 was estimated to be 5 μM. The K_m values for Gln, 2-OG, and ferredoxin were comparable to those of Fd-GOGATs from

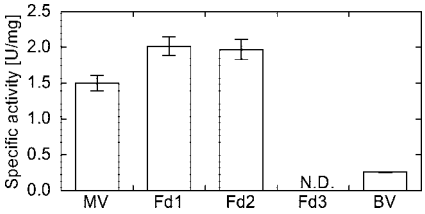

FIG. 6. GOGAT activities with various electron carriers. GOGAT activity was calculated by subtracting the Glu production without electron carriers from that with an electron carrier. Error bars indicate standard errors for at least three independent experiments. MV, methylviologen; BV, benzylviologen; N.D., not detected.

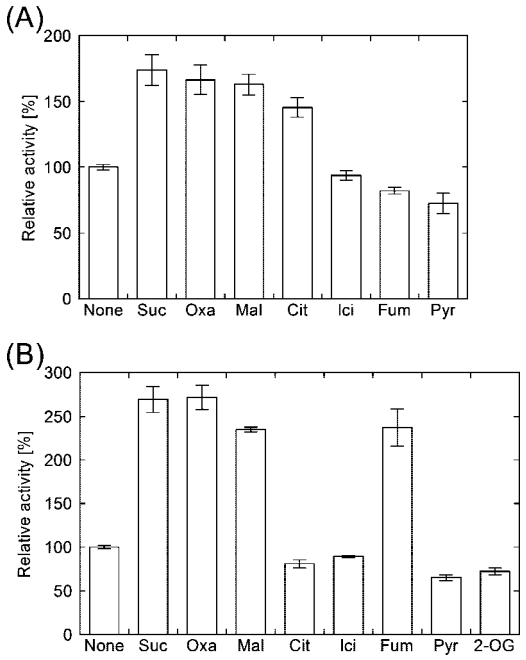

FIG. 7. Relative activities for Glu synthesis under GOGAT assay conditions (A) and glutaminase assay conditions (B) when an organic acid was present in reaction mixtures. The activity of the mixture without any organic acids was designated 100% activity. The following organic acids were added to the mixtures: Suc, succinate; Oxa, oxaloacetate; Mal, malate; Cit, citrate; Ici, isocitrate; Fum, fumarate; and Pyr, pyruvate. Error bars indicate standard errors for at least three independent experiments.

phototrophs (13). The K_m value for Gln was also investigated under the glutaminase assay conditions. In the case of the glutaminase reaction, the K_m value for Gln was estimated to be 2.1 mM, which is approximately twofold higher than the K_m for the GOGAT reaction. The maximal GOGAT activity was detected at 70 to 80°C, which is equivalent to the growth temperature of *H. thermophilus*. Optimum pH was estimated to be 6.9 to 7.4 at 70°C.

Activation by organic acids. Some organic acids that are metabolized in the RTCA cycle were shown to activate purified Fd-GOGAT (Fig. 7A). The presence of 5 mM succinate, oxaloacetate, malate, or citrate caused an increase in Glu production of up to approximately 150% under the Fd-GOGAT assay conditions. In these samples, a stoichiometric increase in the consumption of 2-OG was also detected (data not shown), confirming that the organic acids activated GOGAT activity.

The activating effect of organic acids was also investigated in the glutaminase assay. Under these conditions, Glu production increased in the presence of 5 mM succinate, oxaloacetate, malate, or fumarate (Fig. 7B). Rates of Glu production by these organic acids increased approximately 250%, which is significantly higher than the increase under GOGAT assay conditions. Interestingly, citrate did not activate glutaminase activity, unlike in the case of GOGAT activity, while fumarate activated glutaminase activity but not GOGAT activity. On the other hand, 2-OG and pyruvate inactivated glutaminase activity.

To investigate the concentration dependency for activation, GOGAT and glutaminase activities were measured by varying

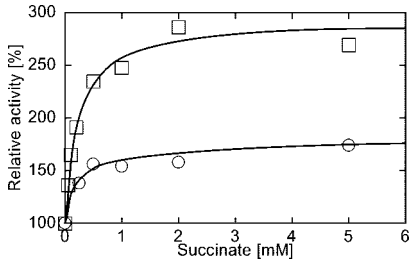

FIG. 8. Relative GOGAT activities (circles) and glutaminase activities (squares) at various succinate concentrations. The activity of mixtures without succinate was designated 100% activity.

the succinate concentration in reaction mixtures (Fig. 8). Succinate causes the activation at low concentrations (below 1 mM) both under GOGAT assay conditions and under glutaminase assay conditions. The addition of two organic acids in combination (succinate, oxaloacetate, malate, or citrate) caused no additive effects on glutaminase activity (data not shown). The presence of succinate and citrate together did not show any synergistic effects on GOGAT activity (data not shown).

DISCUSSION

Fd-GOGAT had been found only in cyanobacteria and plants so far, and it was believed that only phototrophs have Fd-GOGAT. We purified Fd-GOGAT from *H. thermophilus*, a hydrogen-oxidizing chemoautotroph. To the best of our knowledge, this is the first report of Fd-GOGAT from a nonphotosynthetic organism.

In phototrophs that have Fd-GOGAT, ferredoxin participates in photosynthesis and is reduced through photochemical system I. Fd-GOGATs in phototrophs are considered to require photosystem I as the strong ferredoxin-reducing system. In *H. thermophilus*, ferredoxins play a crucial role in the central carbon anabolism pathway, the RTCA cycle. Two key enzymes of the RTCA cycle, pyruvate:ferredoxin oxidoreductase and 2-oxoglutarate:ferredoxin oxidoreductase, utilize ferredoxin as an electron carrier (7, 31). This feature suggests the existence of a strong ferredoxin-reducing system in *H. thermophilus*. This bacterium yields energy and reducing power by molecular hydrogen oxidation, and it is thought that hydrogen oxidation is necessary for ferredoxin reduction. This chemolithotrophic metabolism may play a role equivalent to that of photochemical system I as a ferredoxin-reducing system, making it possible for GOGATs to be of the ferredoxin-dependent type, unlike the case in other bacteria.

Although the amino acid sequence and monomeric structure of the enzyme were similar to those of Fd-GOGATs from phototrophs, some unique characteristics were found. While Fd-GOGATs from many phototrophs have been reported to react with [2Fe-2S] ferredoxins, reactivity with [4Fe-4S] ferredoxins has not been reported so far. In contrast, Fd-GOGAT from *H. thermophilus* reacted with [4Fe-4S] ferredoxins Fd1 and Fd2 but not with the [2Fe-2S] ferredoxin Fd3, indicating that this Fd-GOGAT has a different specificity toward ferredoxins.

Among known Fd-GOGATs, there is a conserved insert region that has been designated the Fd loop. This insertion is present in reported Fd-GOGATs from phototrophs but not in NADPH-GOGATs (Fig. 9) and is presumed to be involved in the interaction with ferredoxin. In contrast, Fd-GOGAT from *H. thermophilus* does not have such a conserved insertion. This fact suggests that the insertion may be dispensable for the interaction with ferredoxin, at least with [4Fe-4S] ferredoxin.

Fd-GOGAT from *H. thermophilus* also has glutaminase activity. There are some reports of NADPH-GOGAT enzymes with glutaminase activity (12, 25), but no Fd-GOGAT has been reported to have glutaminase activity (21). The absence of glutaminase activity can be explained by the sophisticated mechanism of GOGATs, in which the GAT domain is in an active form only when 2-OG and an electron donor are available (26). Our results show that Fd-GOGAT from *H. thermophilus* lacks this mechanism, implying that this enzyme has a slightly different structure from that of other known Fd-GOGATs. Considering the phylogenetically deep origin of *H. thermophilus*, its Fd-GOGAT may be an ancestral type, and the activity regulation at the GAT domain may not have developed in this enzyme.

Fd-GOGAT from *H. thermophilus* is activated by some organic acids. This activation was observed even at low concentrations below 1 mM, suggesting that activation may actually occur in vivo. Glutaminase activity was also increased by some of the organic acids. This result implies that activation was caused by the promotion of Gln hydrolysis at the GAT domain and/or ammonia leakage from the ammonia channel. The absence of additive effects of the organic acids on glutaminase activity suggested that these organic acids bind to the same site in GOGAT for activation. Interestingly, some organic acids, such as citrate and fumarate, have different activation potencies for GOGAT activity and glutaminase activity. This fact

```
                    **  *                                  * ***
Hydrogenobacter     905 EDPERYWTIKN----------------------SAIKQ 920
Synechococcus       900 EDPARFQVLHDVDAEGRSQAFPSIGGLRNGDTACSAIKQ 938
Synechocystis       906 EDVVRYLTLDDVDSEGNSPTLPHLHGLQNGDTANSAIKQ 944
Arabidopsis         902 EDPIRWKPLTDV-VDGYSPTLPHLKGLQNGDIATSAIKQ 939
Spinacia            902 EDPIRWRPLTDV-VDGYSSTLPHLKGLQNGDTATSAIKQ 939
Azospirillum        889 EDPARFRPDKN------------------GDNWNSAIKQ 909
Escherichia         883 EDPARYGTNKV----------------------SRIKQ 898
```

FIG. 9. Amino acid sequences in the vicinity of the Fd loop. Sequences from the following organisms were used: *H. thermophilus*, *Synechococcus* sp. strain WH 8102 (CAE08647), *Synechocystis* sp. strain 6803 (BAA11379), *Arabidopsis thaliana* (AAC78551), *Spinacia oleracea* (AAC26853), *Azospirillum brasilense* (AAA22179), and *Escherichia coli* (BAE77256). Asterisks indicate residues conserved in all seven sequences. The conserved region designated the Fd loop is highlighted in bold. Numbers indicate the positions of amino acid residues counted from the N-terminal Cys residue (position 1).

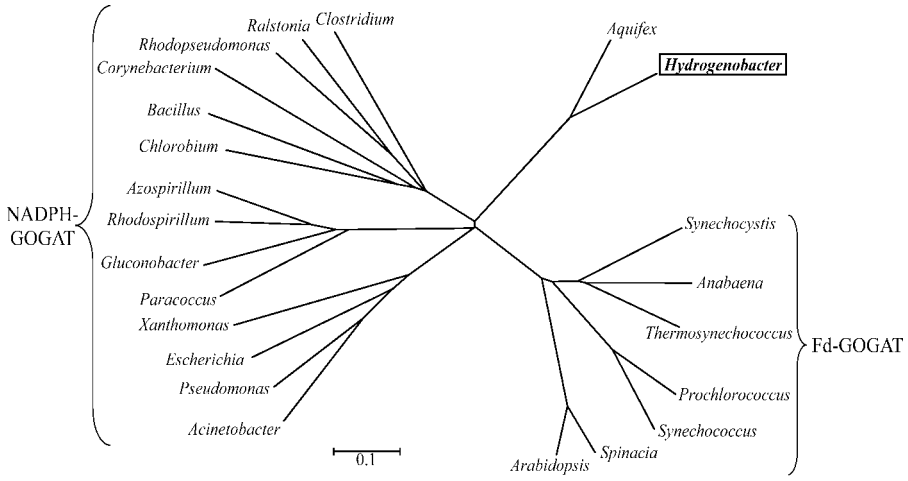

FIG. 10. Phylogenetic tree of Fd-GOGATs and the α subunits of NADPH-GOGAT homologues based on amino acid sequences. Sequences from the following organisms were used: *Acinetobacter* sp. strain ADP1 (CAG70018), *Anabaena variabilis* (ABA20918), *Aquifex aeolicus* (AAC07475), *Arabidopsis thaliana*, *Azospirillum brasilense*, *Bacillus subtilis* (CAB13728), *Chlorobium tepidum* (AAM71647), *Clostridium acetobutylicum* (AAK79639), *Corynebacterium glutamicum* (BAA75929), *Escherichia coli*, *H. thermophilus*, *Gluconobacter oxydans* (AAW61590), *Paracoccus denitrificans* (EAN66504), *Prochlorococcus marinus* (CAE21952), *Pseudomonas aeruginosa* (AAB39259), *Rhodopseudomonas palustris* (CAE26335), *Rhodospirillum rubrum* (ABC20824), *Spinacia oleracea*, *Synechococcus* sp. strain WH 8102, *Synechocystis* sp. strain 6803, *Thermosynechococcus elongatus* (BAC08920), *Xanthomonas campestris* (AAM39351), and *Xylella fastidiosa* (AAO29887).

suggested that these organic acids have activating mechanisms different from those of the other organic acids. However, a synergistic effect of succinate and citrate was not observed, and the activating mechanism remained unclear.

Although GOGATs from some organisms were reported to be inactivated by organic acids (1, 14), to our knowledge activation by organic acids has not been reported. Thus, this activation seems to be a unique feature of Fd-GOGAT from *H. thermophilus*. One of the reasons for this characteristic may be related to the unique form of carbon metabolism in this organism. Since *H. thermophilus* assimilates carbon dioxide through the RTCA cycle, the intracellular concentration of organic acids in this organism is presumed to be more susceptible to the carbon flux than that in other organisms that assimilate carbon through other pathways. Activation by organic acids seems to enable the control of nitrogen assimilation by carbon metabolism.

A phylogenetic tree was constructed using amino acid sequences homologous to that of GltS from *H. thermophilus* (Fig. 10). In this tree, known Fd-GOGATs and NADPH-GOGATs formed one and three branches, respectively. Fd-GOGAT of *H. thermophilus* did not belong to any of these branches; it was located together with the GltS homologue from *A. aeolicus* at a branch isolated from the other enzymes. No other amino acid sequences that belong to this branch were found in the NCBI protein database. This isolated position is consistent with its enzymatic characteristics, which are distinct from those of known NADPH- or Fd-GOGATs, as described above. It is conceivable that the GltS homolog of *A. aeolicus* is not an NADPH-GOGAT because a gene homologous to the β subunit gene of NADPH-GOGAT in its genome is suspected to encode an NAD(P)H oxidoreductase that is unrelated to GOGAT (27). It will be interesting to determine whether the gene product from *A. aeolicus* is an Fd-GOGAT that shares unique characteristics with the *H. thermophilus* enzyme.

This study demonstrated the existence of Fd-GOGAT in a nonphotosynthetic organism and identified characteristics unique to the *H. thermophilus* Fd-GOGAT, providing new insights into GOGAT distribution and enzymatic properties. Structural studies on this enzyme are expected to reveal the type of mechanism that results in these unique properties that differentiate the enzyme from other Fd-GOGATs. The contribution of Fd-GOGAT to total nitrogen assimilation in *H. thermophilus* is also currently under investigation.

ACKNOWLEDGMENTS

This work was partly supported by a grant-in-aid for scientific research from JSPS.

We thank Daijiro Ohmori (Juntendo University) for his help with EPR spectrum measurement.

REFERENCES

1. **Adachi, K., and I. Suzuki.** 1977. Purification and properties of glutamate synthase from *Thiobacillus thioparus*. J. Bacteriol. **129:**1173–1182.
2. **Aoshima, M., M. Ishii, and Y. Igarashi.** 2004. A novel biotin protein required for reductive carboxylation of 2-oxoglutarate by isocitrate dehydrogenase in *Hydrogenobacter thermophilus* TK-6. Mol. Microbiol. **51:**791–798.
3. **Aoshima, M., M. Ishii, and Y. Igarashi.** 2004. A novel enzyme, citryl-CoA synthetase, catalysing the first step of the citrate cleavage reaction in *Hydrogenobacter thermophilus* TK-6. Mol. Microbiol. **52:**751–761.
4. **Aoshima, M., M. Ishii, and Y. Igarashi.** 2004. A novel enzyme, citryl-CoA lyase, catalysing the second step of the citrate cleavage reaction in *Hydrogenobacter thermophilus* TK-6. Mol. Microbiol. **52:**763–770.
5. **Bidlingmeyer, B. A., S. A. Cohen, and T. L. Tarvin.** 1984. Rapid analysis of amino acids using pre-column derivatization. J. Chromatogr. **336:**93–104.
6. **Binda, C., R. T. Bossi, S. Wakatsuki, S. Arzt, A. Coda, B. Curti, M. A. Vanoni, and A. Mattevi.** 2000. Cross-talk and ammonia channeling between active centers in the unexpected domain arrangement of glutamate synthase. Structure **8:**1299–1308.
7. **Ikeda, T., T. Ochiai, S. Morita, A. Nishiyama, E. Yamada, H. Arai, M. Ishii, and Y. Igarashi.** 2006. Anabolic five subunit-type pyruvate:ferredoxin oxidoreductase from *Hydrogenobacter thermophilus* TK-6. Biochem. Biophys. Res. Commun. **340:**76–82.
8. **Ikeda, T., M. Yamamoto, H. Arai, D. Ohmori, M. Ishii, and Y. Igarashi.** 2005. Two tandemly arranged ferredoxin genes in the *Hydrogenobacter thermophilus* genome: comparative characterization of the recombinant [4Fe-4S] ferredoxins. Biosci. Biotechnol. Biochem. **69:**1172–1177.

9. **Ishii, M., S. Takishita, T. Iwasaki, Y. Peerapornpisal, J. Yoshino, T. Kodama, and Y. Igarashi.** 2000. Purification and characterization of membrane-bound hydrogenase from *Hydrogenobacter thermophilus* strain TK-6, an obligately autotrophic, thermophilic, hydrogen-oxidizing bacterium. Biosci. Biotechnol. Biochem. **64:**492–502.
10. **Kameya, M., H. Arai, M. Ishii, and Y. Igarashi.** 2006. Purification and properties of glutamine synthetase from *Hydrogenobacter thermophilus* TK-6. J. Biosci. Bioeng. **102:**311–315.
11. **Koziol, J.** 1970. Fluorometric analyses of riboflavin and its coenzymes. Methods Enzymol. **18B:**253–285.
12. **Mäntsälä, P., and H. Zalkin.** 1976. Glutamate synthase. Properties of the glutamine-dependent activity. J. Biol. Chem. **251:**3294–3299.
13. **Marqués, S., F. J. Florencio, and P. Candau.** 1992. Purification and characterization of the ferredoxin-glutamate synthase from the unicellular cyanobacterium *Synechococcus* sp. PCC 6301. Eur. J. Biochem. **206:**67–77.
14. **Matsuoka, K., and K. Kimura.** 1986. Glutamate synthase from *Bacillus subtilis* PCI 219. J. Biochem. **99:**1087–1100.
15. **Merrick, M. J., and R. A. Edwards.** 1995. Nitrogen control in bacteria. Microbiol. Rev. **59:**604–622.
16. **Meyer, J., M. D. Clay, M. K. Johnson, A. Stubna, E. Münck, C. Higgins, and P. Wittung-Stafshede.** 2002. A hyperthermophilic plant-type [2Fe-2S] ferredoxin from *Aquifex aeolicus* is stabilized by a disulfide bond. Biochemistry **41:**3096–3108.
17. **Nalbantoglu, B., M. Hirasawa, C. Moomaw, H. Nguyen, D. B. Knaff, and R. Allen.** 1994. Cloning and sequencing of the gene encoding spinach ferredoxin-dependent glutamate synthase. Biochim. Biophys. Acta **1183:**557–561.
18. **Oliver, G., G. Gosset, R. Sanchez-Pescador, E. Lozoya, L. M. Ku, N. Flores, B. Becerril, F. Valle, and F. Bolivar.** 1987. Determination of the nucleotide sequence for the glutamate synthase structural genes of *Escherichia coli* K-12. Gene **60:**1–11.
19. **Pelanda, R., M. A. Vanoni, M. Perego, L. Piubelli, A. Galizzi, B. Curti, and G. Zanetti.** 1993. Glutamate synthase genes of the diazotroph *Azospirillum brasilense*. J. Biol. Chem. **268:**3099–3106.
20. **Pitulle, C., Y. Yang, M. Marchiani, E. R. B. Moore, J. L. Siefert, M. Aragno, P. Jurtshuk, Jr., and G. E. Fox.** 1994. Phylogenetic position of the genus *Hydrogenobacter*. Int. J. Syst. Bacteriol. **44:**620–626.
21. **Ravasio, S., L. Dossena, E. Martin-Figueroa, F. J. Florencio, A. Mattevi, P. Morandi, B. Curti, and M. A. Vanoni.** 2002. Properties of the recombinant ferredoxin-dependent glutamate synthase of *Synechocystis* PCC6803. Comparison with the *Azospirillum brasilense* NADPH-dependent enzyme and its isolated α subunit. Biochemistry **41:**8120–8133.
22. **Reitzer, L.** 2003. Nitrogen assimilation and global regulation in *Escherichia coli*. Annu. Rev. Microbiol. **57:**155–176.
23. **Shiba, H., T. Kawasumi, Y. Igarashi, T. Kodama, and Y. Minoda.** 1982. The deficient carbohydrate metabolic pathways and the incomplete tricarboxylic acid cycle in an obligately autotrophic hydrogen-oxidizing bacterium. Agric. Biol. Chem. **46:**2341–2345.
24. **Shiba, H., T. Kawasumi, Y. Igarashi, T. Kodama, and Y. Minoda.** 1985. The CO_2 assimilation via the reductive tricarboxylic acid cycle in an obligately autotrophic, aerobic hydrogen-oxidizing bacterium, *Hydrogenobacter thermophilus*. Arch. Microbiol. **141:**198–203.
25. **Trotta, P. P., K. E. B. Platzer, R. H. Hascemeyer, and A. Meister.** 1974. Glutamine-binding subunit of glutamate synthase and partial reactions catalyzed by this glutamine amidotransferase. Proc. Natl. Acad. Sci. USA **71:**4607–4611.
26. **van den Heuvel, R. H. H., D. Ferraro, R. T. Bossi, S. Ravasio, B. Curti, M. A. Vanoni, F. J. Florencio, and A. Mattevi.** 2002. Structural studies on the synchronization of catalytic centers in glutamate synthase. J. Biol. Chem. **277:**24579–24583.
27. **Vanoni, M. A., and B. Curti.** 1999. Glutamate synthase: a complex iron-sulfur flavoprotein. Cell. Mol. Life Sci. **55:**617–638.
28. **Vanoni, M. A., L. Dossena, R. H. H. van den Heuvel, and B. Curti.** 2005. Structure-function studies on the complex iron-sulfur flavoprotein glutamate synthase: the key enzyme of ammonia assimilation. Photosynth. Res. **83:**219–238.
29. **Vanoni, M. A., D. E. Edmondson, M. Rescigno, G. Zanetti, and B. Curti.** 1991. Mechanistic studies on *Azospirillum brasilense* glutamate synthase. Biochemistry **30:**11478–11484.
30. **Yamamoto, M., H. Arai, M. Ishii, and Y. Igarashi.** 2003. Characterization of two different 2-oxoglutarate:ferredoxin oxidoreductases from *Hydrogenobacter thermophilus* TK-6. Biochem. Biophys. Res. Commun. **312:**1297–1302.
31. **Yoon, K. S., M. Ishii, T. Kodama, and Y. Igarashi.** 1997. Carboxylation reactions of pyruvate:ferredoxin oxidoreductase and 2-oxoglutarate:ferredoxin oxidoreductase from *Hydrogenobacter thermophilus* TK-6. Biosci. Biotechnol. Biochem. **61:**510–513.
32. **Zanetti, G., C. Binda, and A. Aliverti.** 2001. The [2Fe-2S] ferredoxins, p. 532–542. *In* A. Messerschmidt, R. Huber, T. Poulos, and K. Wieghardt (ed.), Handbook of metalloproteins. John Wiley & Sons, Chichester, United Kingdom.